JOURNAL OF CATALYSIS 75, 302–313 (1982)

The Catalytic Reactions of CO and H_2O over Supported Rhodium

MIKI NIWA AND JACK H. LUNSFORD

Department of Chemistry, Texas A&M University, College Station, Texas 77843

Received July 28, 1981; revised December 23, 1981

Reactions of CO with H_2O over supported rhodium to form H_2, CH_4, and CO_2 were studied. The formation of methane appears to occur via the water gas shift reaction, followed by the hydrogenation of surface carbon. By operating at sufficiently small contact times it was possible to follow only the water gas shift reaction. The turnover frequency for this reaction was a function of the type of support, resulting in the turnover frequency sequence: Rh/Al_2O_3 > Rh/Y zeolite > Rh/SiO_2 > RhNaY zeolite. This sequence correlates with the activity of supported rhodium in the formation of surface carbon. On the basis of this relationship and kinetic data it appears that surface carbon is an important intermediate in the water gas shift reaction. By contrast, a previous study indicated that over supported ruthenium the principal reaction mechanism involved molecular rather than dissociated CO. The turnover frequencies observed with supported Rh were more than an order of magnitude less than those observed with supported Ru.

INTRODUCTION

The catalytic reaction of water with carbon monoxide to form hydrocarbons and carbon dioxide, known as the Kölbel–Engelhardt reaction (*1*) provides a single-step process for hydrocarbon synthesis. Although there are reports which suggest that CO may react directly with adsorbed H_2O or OH^- to form CH_4 (*2, 3*), most catalytic work indicates that the Kölbel–Engelhardt reaction itself is in fact a water gas shift (WGS) reaction followed by a Fischer–Tropsch (FT) reaction (*4, 5*). Thus, as a suitable catalyst for the Kölbel–Engelhardt reaction one must have a material which is active both for the WGS and the FT reactions.

Supported group VIII metals have been extensively studied as FT and methanation catalysts (*6*); however, their role in the WGS reaction is less well understood. The catalytic reactions of CO and H_2O over ruthenium supported on alumina, silica, and in a Y-type zeolite have been recently studied (*4*). Moreover, preliminary work on the Kölbel–Engelhardt reaction over a RhY zeolite has been reported (*7*). In the present investigation the WGS and methanation reactions have been studied separately and in concert for the Kölbel–Engelhardt reaction.

Zeolites were selected as a support to further explore the effects on catalytic activity which result from restricting small metal particles within the 13-Å cavities. By variations in preparation techniques it also has been possible to compare properties of the metal particles either within or on the external surface of a zeolite.

Surface carbon plays a much more important role in the WGS reaction over supported rhodium than over supported ruthenium. In addition, the disproportionation of CO to form this surface carbon depends upon the type of support. The latter results are consistent with current evidence which suggests that the dissociation of CO on rhodium surfaces requires the presence of irregularities including steps, kinks, and defects (*8*). It is anticipated that the concentration of these irregularities would depend upon the nature of the support. Since the WGS reaction over ruthenium appears to proceed mainly via molecular CO, the imperfections are not critical and the

0021-9517/82/060302-12$02.00/0

turnover frequencies observed with ruthenium on the three supports were remarkably similar (*4*).

EXPERIMENTAL METHODS

Catalysts and Chemicals

As will be subsequently demonstrated, the exchange of metal ions either uniformly throughout the zeolite crystallites or predominantly on the external surface can be achieved by employing different rhodium salts. In order to achieve uniform exchange 3 g of NaY zeolite (Linde, lot no. 3365-94) was introduced to a 3.5-liter solution of $[Rh(NH_3)_5Cl]Cl_2$ at a pH of ca. 4. Ion exchange was carried out at 80°C. One sample was prepared with a CaY zeolite as the starting material. These catalysts will be designated as RhNaY or RhCaY zeolites. When the ion exchange was carried out in a solution of $Rh(NO_3)_3 \cdot 2H_2O$, with all other conditions the same, the metal ions were located predominantly on the external surface of the NaY zeolite. These materials are designated as Rh/Y.

The Rh/Al_2O_3 and Rh/SiO_2 catalysts, containing 2 wt% rhodium, were prepared by impregnation of Al_2O_3 (CONOCO Catapal) and SiO_2 (Davison SMR 7-5519) with a solution of 7.3×10^{-4} *M* rhodium nitrate. A 1.0-liter solution with 3.0 g of the solid phase was evaporated to dryness.

Carbon monoxide (99.99%), helium (99.995%), and hydrogen (99.999%) were obtained from Matheson. The O_2 impurity of these gases was further reduced by passing them through a Cr^{II}/SiO_2 column.

Apparatus and Procedure

Kinetic data were obtained both in a single-pass flow reactor and in a recirculating reactor. Both reactors were constructed of glass. The reactants were introduced to the single-pass flow reactor after bubbling a mixture of helium and carbon monoxide through water. The partial pressure of water was controlled by passing the gas mixture through a volume at a predetermined temperature. The W/F (weight of catalyst/total flow rate) values are reported at 25°C. The recirculating reactor was part of a 248-cm^3 closed-loop system which contained a glass pump.

The catalysts were pretreated by first heating the materials under vacuum at 25°C for 1 h, at 100°C for 1 h and in 100°C increments to 400°C for 1 h. The RhNaY and RhCaY catalysts were oxidized at 400°C for 1 h. All catalysts were reduced at 400°C in 200 Torr of recirculating H_2 for 16 h with a cold trap in the system.

The gas phase reactants and products were analyzed by on-line chromatography. A porapak Q column at 70°C was used for the separation of CO, CH_4, and CO_2. Hydrogen was separated over a 13X molecular sieve column at 25°C and was oxidized to H_2O over CuO before entering the thermal conductivity detector. The oxidation step greatly enhanced the sensitivity for H_2.

Chemisorption of H_2 and CO

Adsorbed amounts of H_2 and CO were measured volumetrically following catalyst reduction. Used catalysts were reduced with hydrogen for 2 h at 400°C and heated under vacuum for 2 h at that temperature. The adsorption isotherm for hydrogen was obtained in the range 100–400 Torr, and the amount of adsorbed H_2 was measured by extrapolating the linear portion of the isotherm to zero pressure (*9*).

With CO one adsorption isotherm which included both physically and chemically adsorbed CO was determined, and the sample volume was evacuated for 2 min at 25°C. A second isotherm which included only physically adsorbed CO was determined, and the difference between the two isotherms at 100 Torr was taken as the amount of chemisorbed CO.

Infrared and Photoelectron Spectroscopy

Infrared spectra were recorded using a Beckman IR-9 spectrophotometer, which was usually operated in the transmission mode. Self-supporting zeolite wafers were formed under a pressure of 1500 kg/cm^2.

The X-ray photoelectron spectra (XPS) were obtained on similar wafers with a Hewlett–Packard Model 5950A spectrometer. The Si_{2s} line at 154.0 eV and the C_{1s} line at 285.0 eV were used as internal standards to determine binding energies. The Rh/Si ratios were based on the areas of the $Rh_{3d_{5/2}}$ line and the Si_{2p} line with appropriate corrections for the cross sections (*10*).

RESULTS AND DISCUSSION

Catalyst Characterization

Temperature-programmed reduction. In order to evaluate the extent of reduction of the supported rhodium temperature-programmed reduction (TPR) experiments were carried out in the recirculating reactor. Since Rh^{III} was reduced to Rh^{I} by heating under vacuum at elevated temperatures (*11, 12*), the samples used in this experiment were heated in 50 Torr O_2 at 500°C for 2 h and cooled to 25°C. After evacuation of gas phase O_2 for ca. 10 min at 25°C, 50 Torr of H_2 was circulated as the catalyst was heated at a rate of 2°C/min. The gas phase H_2 was periodically analyzed, and the molecules of H_2 reacted or produced per Rh atom as a function of temperature is depicted in Fig. 1.

The reduction of rhodium oxide can be described by the stoichiometric equations

$$RhO_n + \left(n + \frac{x}{2}\right)H_2 \rightarrow RhH_x + nH_2O, \quad (1)$$

$$RhH_x \rightarrow Rh + \frac{x}{2}H_2. \quad (2)$$

The value of n is the difference between the H_2 uptake and the desorbed amount of H_2.

The results of Fig. 1 show that H_2 reacted with the oxide at temperatures between 50 and 100°C, with 2 wt% RhNaY being the most active. At temperatures between 200 and 400°C hydrogen was evolved from the catalysts. A value of $n = 1.5 \pm 0.2$ was obtained for the three catalysts, which is consistent with an initial oxidation state of Rh^{III} and a final oxidation state of Rh^0. The

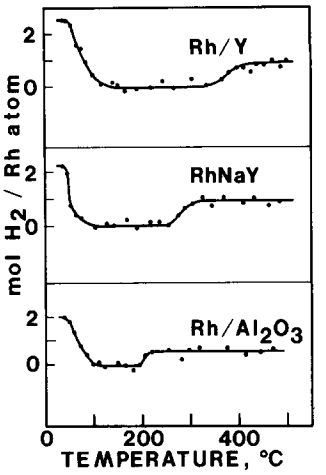

FIG. 1. Temperature programmed reduction of supported rhodium catalysts. Catalysts were heated at 2°C/min in H_2 (P^o = 50 Torr).

amount of hydrogen evolved at 200–400°C suggests that RhH_2 is stabilized on the two zeolites; whereas, RhH is stabilized on Al_2O_3.

Yao *et al.* (*13*) carried out TPR experiments on Rh/Al_2O_3 catalysts, but they did not observe the high-temperature evolution of H_2, possibly because their rate of temperature increase (10°C/min) was quite large. In the TPR of $PtRe/Al_2O$ studied by Wagstaff and Prins (*14*), the reduction of the catalyst and the evolution of H_2 were clearly separated. The results indicated a PtH phase.

Chemisorption of H_2 and CO. After exposure to CO and H_2O at 370°C in the flow reactor the amounts of chemisorbed H_2 and CO were determined. The results listed in Table 1 show that except for the 0.5 wt% Rh/Y and the 2 wt% Rh/SiO_2 sample the dispersions, as determined from hydrogen chemisorption, were appreciable. For the 2 wt% catalysts these values indicate an average Rh particle size of 29, 25, and 15 Å for Rh/Y, RhNaY, and Rh/Al_2O_3. An average particle size of ca. 25 Å was determined for RuNaY, both by H_2 chemisorption and by transmission electron microscopy, even though the ruthenium was shown to be within the zeolite crystallites (*4*). The pres-

TABLE 1

Chemisorption Data and Activities of Supported Rhodium Catalysts in the Continuous Flow Reactor

Catalyst	H_2 Chemisorption (μmol/g-cat)[a]	CO Chemisorption (μmol/g-cat)[a]	Activity (mmol/h · g-cat)[b]			
			H_2	CH_4	C_2H_6	CO_2
Rh/Y 4 wt%	76 (39)	43	2.24	2.13	0.0	7.67
2 wt%	39 (40)	27	1.43	1.16	0.0	4.67
1 wt%	32 (66)	—	1.28	0.13	0.0	1.84
0.5 wt%	19 (78)	—	0.0	0.0	0.0	0.0
RhNaY[c] 2 wt%	44 (45)	18	1.09	0.09	0.0	1.47
RhNaY 2 wt%	— —	—	1.01	0.01	0.0	0.99
RhCaY[c] 2 wt%	37 (38)	—	0.75	0.03	0.0	1.01
Rh/Al_2O_3 2 wt%	76 (78)	101	4.74	0.61	0.03	6.23
Rh/SiO_2 2 wt%	6.7 (7)	12	0.71	0.0	0.0	0.70
Al_2O_3	— —	—	0.05	0.0	0.0	0.04

[a] Used catalyst; values for dispersion are given in parentheses.

[b] Obtained over 0.38 g of the catalyst at 370°C. P_{CO}° = 84 Torr. $P_{H_2O}^{\circ}$ = 26 Torr, and contact time W/F = 0.014 g · min/ml. Activity is expressed per total mass of catalyst.

[c] Oxidized with O_2, and then reduced with H_2 at 400°C.

ence of particles of this size within the 13-Å cavities of the zeolite was attributed to agglomeration of the metal in several adjacent supercages such that the particles are connected through the 12-membered windows (*15*).

Except for the Rh/SiO_2 catalyst the CO/H ratio and thus the CO/Rh ratio was appreciably less than unity. This is consistent with the infrared results (see below) which will confirm that $Rh(CO)_2$ complexes are not prevalent on the used catalysts.

X-Ray photoelectron spectroscopy. The XPS results for both fresh and used catalysts are summarized in Table 2. The values of 312.2–312.3 eV for the $Rh_{3d_{3/2}}$ line and 307.3–307.6 for the $Rh_{3d_{5/2}}$ line are consistent with, but do not prove, the existence of Rh^0. The problem in distinguishing the Rh^0 and Rh^I oxidation states comes about because of the small differences in binding energies. For example, Rh^0 as the metal has binding energies of 312.1 and 307.2 eV (*12, 16*) while Rh^I in $[Rh^I(CO)_2Cl]_2$/NaY has values of 312.4 and 307.8 eV (*17*). When one considers an error of ±0.2 eV and the possible matrix effects, it is difficult to distinguish between these two oxidation states with any degree of confidence.

The XPS data, however, provide convincing evidence that the rhodium in the Rh/Y zeolites is mainly on the external surface of the crystallites. The Rh/Si ratios were a factor of 5–7 times greater than the theoretical ratios, assuming uniform exchange; whereas, for the RhNaY sample the Rh/Si ratios are essentially equivalent to the theoretical values. These results confirm the conclusions of Okamoto *et al.* (*12*) and Iizuka and Lunsford (*11*) that ion

TABLE 2

XPS Data for Rhodium Catalysts

Catalyst		Binding energy (eV) Rh_{3d} 3/2	5/2	(Rh/Si) exptl.	(Rh/Si) theoretical
Rh/Y	Fresh	312.3[a]	307.6	0.13	0.018
	Used	312.2[a]	307.4	0.083	0.018
RhNaY	Fresh	312.1[a]	307.3	0.023	0.020
	Used	312.1[a]	307.3	0.019	0.020
Rh/Al_2O_3	Used	312.1[b]	307.4	—	—

[a] Calculated using the Si_{2s} line (154.0 eV) as a standard.

[b] Calculated using the C_{1s} line (285.0 eV) as a standard.

exchange using a rhodium salt in solution ($RhCl_3$ or $Rh(NO_3)_3$) leads to a high concentration of metal ions on the external surface of the zeolite. Uniform exchange must be inhibited by the formation of polynuclear complexes, even at the relatively low cation concentration and pH employed in these experiments.

Infrared spectroscopy. Carbon monoxide adsorbed on supported rhodium has been extensively studied by infrared techniques (*18–20*). The infrared spectra are commonly assigned to three carbonyl species: (1) a linear RhCO monocarbonyl characterized by a single band which may occur at wavenumbers from 2075 to 2000 cm^{-1}, depending on the particle size and surface coverage; (2) a bridged Rh_2CO monocarbonyl which gives rise to a broadband having wavenumbers between 1900 and 1850 cm^{-1}; and (3) a partially oxidized dicarbonyl $Rh(CO)_2$ characterized by a doublet with bands in the range 2120–2100 and 2030–2020 cm^{-1}. Both comparisons with model compounds and chemical evidence suggest that the dicarbonyl is actually present as a $Rh^{I}(CO)_2$ complex (*21*). This is particularly interesting since it is the dominant form of carbonyl complexes following the adsorption of CO on a fresh, well-reduced RhY zeolite, which indicates, as Primet (*21*) has pointed out, that CO dissociates on small rhodium particles, giving rise to Rh^{I}.

Adsorption of CO on both the Rh/Y and RhNaY zeolites resulted in two dicarbonyl complexes with pairs of bands at 2118 and 2050 cm^{-1} and at 2100 and 2025 cm^{-1} in good agreement with the results of Primet (*21*). The origin of the differences between the two complexes has not been adequately explained; however, Smith *et al.* (*22*) have attributed similar shifts in frequency for rhodium carbonyl complexes on alumina to hydrogen bonding between hydroxyl groups and carbonyl groups. The $Rh^{I}(CO)_2$ complexes in the zeolite were stable *in vacuo* up to about 150°C and were completely decomposed by 250°C.

Although the dicarbonyl spectra on the RhNaY and Rh/Y zeolites were quite similar, with the latter material a moderately sharp band was also observed at 1828 cm^{-1} and absorption in the region 2050–2100 cm^{-1} was apparent. These bands are in agreement with those found for the $Rh_6(CO)_{16}$ complex on Al_2O_3 (*22*) (2058, 1830 cm^{-1} for Al_2O_3 pretreated at 200°C), and suggest that this cluster compound may be formed in the zeolite from small rhodium particles. It should be noted that Primet (*21*) observed rhodium particles from 4–8 Å by electron microscopy with comparable RhY zeolites.

After exposing the catalysts to CO and H_2O under reaction conditions, followed by subsequent evacuation and readdition of CO the spectra depicted in Fig. 2 were observed. Remnants of the $Rh^{I}(CO)_2$ spectra are evident with the zeolites; however, the dominant feature is that of linear CO on Rh^0. The bands were at 2050 and 2065 cm^{-1} for RhNaY and Rh/Y, respectively. The differences in the wavenumbers may reflect the rhodium particle size or more likely the effect of the zeolite on the electronic struc-

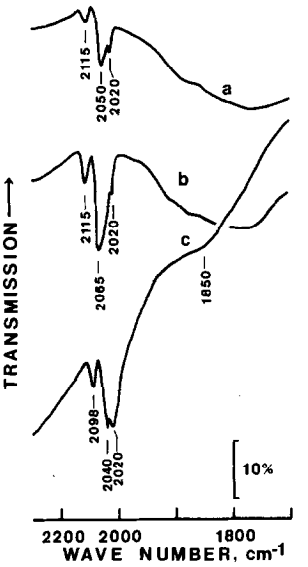

FIG. 2. Infrared spectra of CO adsorbed on supported rhodium catalysts: (a) RhNaY, (b) Rh/Y, (c) Rh/Al_2O_3.

ture of the particle. There is no clear evidence in the spectra for bridging carbonyls.

By contrast the broadband at 1850 cm^{-1} observed with the Rh/Al_2O_3 catalyst is due to bridging carbonyls. The band at 2020 cm^{-1} is probably a combination of the linear monocarbonyl species and one mode of the dicarbonyl species, with the other mode being at 2098 cm^{-1}. The weak, but sharp, shoulder at 2040 cm^{-1} is probably due to another set of monocarbonyl complexes.

Kinetic Studies

Steady-state results. The product distribution as a function of temperature for a 4 wt% Rh/Y catalyst is given in Fig. 3. It is evident from these results that at temperatures below 335°C the concentrations of CO_2 and H_2, formed by the WGS reaction

$$CO + H_2O \rightleftarrows H_2 + CO_2, \qquad (3)$$

were essentially equivalent with almost no CH_4 being formed. In fact, at sufficiently small W/F values the production of CH_4 was reduced to zero while the WGS reaction was proceeding at a reasonable rate. Upon raising the temperature of the catalyst or increasing the contact time methane was produced by the reaction

$$2CO + 2H_2 \rightarrow CH_4 + CO_2. \qquad (4)$$

Since substantial amounts of hydrogen were present in the gas phase there is no reason to propose a direct reaction of H_2O or OH^- with surface carbon or adsorbed CO to produce the observed methane.

Under the conditions of this experiment (84 Torr CO and 26 Torr H_2O) water is the limiting reagent, thus when the water was essentially all consumed the steady-state hydrogen production decreased as more methane was formed. Although the concentration of H_2O was not determined directly, the amount remaining may be evaluated from a material balance, and it is evident that the WGS reaction was essentially at equilibrium by 370°C.

The product distributions under conditions of constant temperature and W/F are compared in Table 1. Several qualitative observations can be made from these results. First, methane was the only hydrocarbon detected over rhodium supported in the zeolites or on silica, but small amounts of ethane were detected over rhodium on alumina. The Rh/Al_2O_3 catalyst was the most active for the WGS reaction but was less active in CH_4 formation than a comparable 2 wt% Rh/Y catalyst. Moreover, uniformly exchanged 2 wt% RhNaY and RhCaY catalysts were less active for both the WGS reaction and the methanation reaction. The activities of the Rh/Y zeolites depended very much on the wt% Rh, with the 0.5 wt% sample showing no activity for either reaction. The anomalous loss of activity may be related to the particle size of the rhodium. For example, Gelin *et al.* (*23*) have observed that the decomposition of $Rh_6(CO)_{16}$ in NaY zeolites resulted in cluster integrity only in samples with low rhodium content (0.5 wt% RhNaY). Thus, the cluster size in the 0.5 wt% Rh/Y samples may be less than that required for CO activation. Although the active Rh/Al_2O_3 catalyst has a similar dispersion, it is likely that the topology of the metal on the two catalysts is quite different. Yates *et al.* (*20*) have presented convincing evidence that

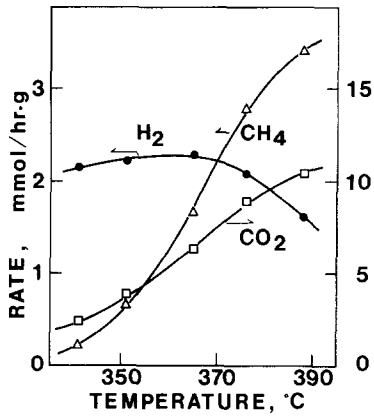

FIG. 3. Product distribution at steady state as a function of temperature over a 4 wt% Rh/Y catalyst: P_{CO}^0 = 84 Torr, $P_{H_2O}^0$ = 26 Torr, W/F = 0.014 g · min/ml.

rhodium is dispersed on alumina in the form of rafts.

Since the WGS reaction is known to occur over alumina (*25*), blank experiments on the support were carried out. Under our experimental conditions the activity of Al_2O_3 for the WGS reaction was two orders of magnitude less than the Rh/Al_2O_3 sample. In addition, the activity for the WGS reaction over an unreduced RhNaY catalyst was found to be negligible, unlike the case of ionic ruthenium complexes in zeolites, which are some of the most active catalysts known for the WGS reaction (*25*).

At small W/F values it was possible to obtain kinetic parameters for the WGS reaction without the complication of a subsequent methanation reaction. For comparison with literature values the methanation reaction, using H_2 as the source of hydrogen, was also studied. The results given in Table 3 show that the order of the WGS reaction is ca. -0.15 to -0.3 with respect to CO and ca. 0.5 with respect to H_2O. These values may be compared with those obtained for the WGS reaction over supported ruthenium for which orders of -0.87 and 0.6 for CO and H_2O, respectively, were obtained (*4*). For the various supports the turnover frequencies (TOF) are in the order Rh/Al_2O_3 > 4 wt% Rh/Y > Rh/SiO_2 > RhNaY. The sixfold difference in TOF between the most active and the least active catalyst is in contrast with supported ruthenium catalysts for which the variation was only a factor of 1.5, with Ru/SiO_2 being the most active and RuY being the least active catalyst (*4*).

The turnover frequencies for the methanation reaction exhibited much less variation, and were only a factor of 2 to 3 greater than the extrapolated value obtained for Rh/Al_2O_3 by Vannice (*26*). This also is in contrast with the supported ruthenium, for which the TOF for methanation appears to be dependent upon the metal particle size (*26–28*). These differences, both with respect to the methanation reaction and more particularly the WGS reaction, may be related to variations in the mechanism or the rate-limiting step, as will be subsequently discussed.

Transient results. Upon carrying out the reaction in the recirculation reactor initial results on a freshly pretreated catalyst could be obtained. The data qualitatively agree with the results of the flow experiments; i.e., at short reaction times only the WGS reaction was observed while at longer reaction times methane was produced. The origin of this induction period for methane has been explored by varying the pretreatment conditions. The standard pretreatment gave the results of curve 1 in Fig. 4;

TABLE 3

Reaction Orders and Turnover Frequencies for the Water Gas Shift Reaction and Methanation Reactions

Catalyst	WGS			Methanation		
	Reaction order[a]		TOF[b]	Reaction order[c]		TOF[d]
	n	m	($N(\times 10^3)$ sec^{-1})	n	m	($N(\times 10^3)$ sec^{-1})
Rh/Y 4 wt%	−0.17	0.56	19	−0.48	1.3	18
RhNaY	−0.14	0.43	7.8	—	—	18
Rh/Al_2O_3	−0.32	0.45	50	−0.45	1.3	27
Rh/SiO_2	—	—	16	—	—	—

[a] Defined as $r = k_1 P_{CO}{}^n P_{H_2O}{}^m$.
[b] Obtained at 350°C, $P_{CO}{}^0 = 55$ Torr and $P_{H_2O}{}^0 = 26$ Torr.
[c] Defined as $r = k_2 P_{CO}{}^n P_{H_2}{}^m$.
[d] Obtained at 300°C, $P_{CO}{}^0 = 43$ Torr and $P_{H_2}{}^0 = 122$ Torr.

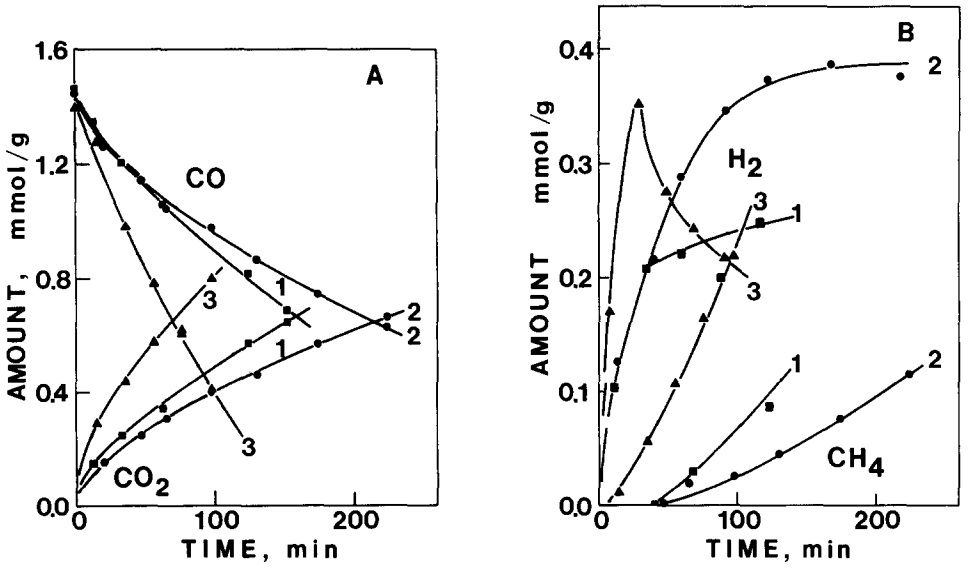

FIG. 4. Product distribution as a function of time in recirculating reactor over a 2 wt% Rh/Y catalyst at 318°C; P_{CO}° = 22 Torr, $P_{H_2O}^{\circ}$ = 15 Torr: (A) CO and CO_2, (B) H_2 and CH_4. (1) After standard pretreatment and several reactions, (2) sample pretreatment with H_2O at 318°C, (3) sample pretreated by heating *in vacuo* at 500°C.

whereas, pretreatment with H_2O at 318°C resulted in a substantially longer induction period (curve 2). Evacuation of the sample at 500°C for 3 h caused a much more rapid increase in the amount of H_2 and the induction period for methane likewise decreased (curve 3). In a separate experiment 23 Torr H_2 was added to the CO/H_2O mixture and the reaction was carried out at 292°C. Under these conditions no induction period was observed, and, in addition, a small amount of ethane was produced.

A similar induction period for methane formation was observed over the RuY catalyst, and it was found that the induction period became negligible when $P_{H_2}^{\circ}/P_{H_2O}^{\circ} \simeq 0.8$. These results suggest that during the initial stages of the WGS reaction the amount of H_2 produced is not able to compete with H_2O for adsorption sites, but as more H_2 is formed and H_2O is consumed a sufficient amount of H_2 is activated for the methanation reaction to occur.

The very selective formation of CH_4 as the only hydrocarbon produced when CO and H_2O reacted over a Rh/Y zeolite led us to speculate in the preliminary report that CO_2, rather than CO, was somehow being hydrogenated (*7*). More recent results, however, indicate that the hydrogenation of CO_2 occurs through its dissociation to CO and then to surface carbon (*29*). Moreover, as depicted in Fig. 5, with a mixture of CO, CO_2, and H_2 the CO first is consumed and then CO_2 is consumed. Since in the absence of CO the TOF for CH_4 formation from CO_2 is actually greater than that from CO (*29*), some CH_4 indeed may be coming from CO_2

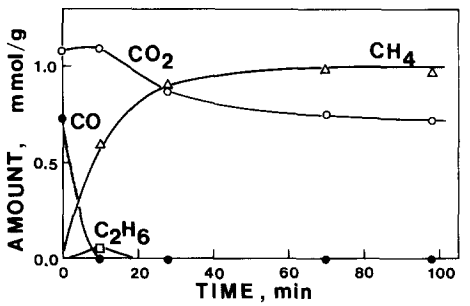

FIG. 5. Competitive reactions in recirculating reactor over a 2 wt% Rh/Y catalyst at 275°C. P_{CO}° = 11 Torr, $P_{CO_2}^{\circ}$ = 17 Torr, $P_{H_2O}^{\circ}$ = 54 Torr.

in the present experiment; however, the *net* consumption of CO_2 is negligible until all of the CO is consumed. The transient formation of C_2H_6 will be discussed in the next section.

Mechanistic Studies

Since one of the fundamental objectives of this study was to determine whether the formation of methane occurred via the WGS reaction or by some more direct pathway, sequential reactions were carried out in which the Rh/Y catalyst was first exposed to CO and then to either H_2O or H_2. The data, shown in Fig. 6, confirm that CO does disproportionate over the supported rhodium. Although similar results have been reported (*30*), the observation is interesting in view of the controversy over the disproportionation, or more correctly the dissociation, of CO on single crystal surfaces. Recent results by Yates *et al.* (*31*) suggest that the dissociation of CO does not occur on the Rh(111) face of rhodium; however, Somorjai and co-workers (*8, 32*) have shown that the reaction does occur at step or defect sites on single crystals and on polycrystalline rhodium films. Presumably these surface irregularities are abundant on supported rhodium crystallites, and their concentrations may vary from one support to another.

Following the removal of carbon monoxide, water was recirculated over the carbon-containing Rh/Y catalyst, and as indicated in Fig. 6, only H_2 and CO_2 were formed. Under these conditions no CH_4 was detected; however, after the sample was heated *in vacuo* at ca. 320°C and subsequently exposed to 50 Torr of H_2 a small amount of CH_4 was observed. If 50 Torr of H_2 was added first an appreciable amount of methane was formed, and subsequent addition of H_2O resulted in only small amounts of H_2 and CO_2.

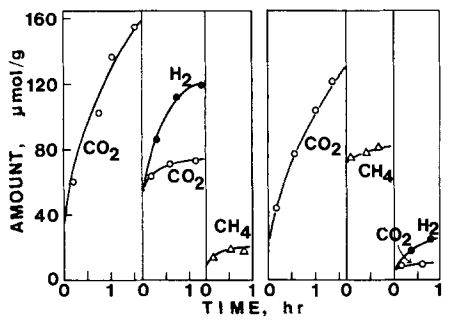

FIG. 6. Products observed during disproportionation of CO and following reaction of the 4 wt% Rh/Y catalyst with H_2O and H_2; $P_{H_2}^{\circ}$ = 50 Torr, $P_{H_2O}^{\circ}$ = 25 Torr, T = 320°C.

Quantitative results for the same series of reactions, carried out on this and other catalysts, are listed in Table 4. The same products were observed for all of the catalysts except for Rh/Al_2O_3 which yielded CH_4 upon reacting H_2O with the surface carbon. This may be attributed to the formation of considerably more H_2 and surface carbon. The RhNaY catalyst was also unusual in that the total amount of carbon recovered as CO_2 and CH_4 exceeded the amount of surface carbon estimated from the amount of CO_2 formed during the disproportionation reaction. This phenomenon, which was also observed for RuY catalysts, has been attributed to the formation of carbon by the dissociation reaction and the movement of the oxygen within the metal crystallite (*33*).

Gupta *et al.* (*34*) have previously noted that the surface carbon is converted with time to an inactive form. This is substantiated with the 4 wt% Rh/Y sample which was allowed to stand for 1 h at 314°C after the disproportionation reaction. Only 16% of the surface carbon was reacted on this sample upon exposure to H_2O; whereas, 50% of the surface carbon was reacted when the sample was immediately exposed to H_2O following removal of excess CO.

Although the amount of CO_2 derived from the disproportionation reaction may be somewhat misleading, it serves as a useful lower-limit estimate of the amount of surface carbon. The concentration of CO_2 produced by the disproportion of CO was determined as a function of time at 328°C, and the results are shown in Fig. 7. Upon

TABLE 4

Reaction of H_2O and H_2 with Surface Carbon

Catalyst	T (°C)	Products (μmol/g-cat)											
		CO[a]	H_2O[a]			H_2[a]	Total recovery[c]	CO[a]	H_2[a]		H_2O[a]		Total recovery[c]
		C_{ads}[b]	CO_2	H_2	CH_4	CH_4		C_{ads}[b]	CH_4	CO_2	H_2	CH_4	
Rh/Y 4 wt%	313	160	79	128	0	20	99	128	85	11	23	0	96
	314[d]	179	28	43	0	7	35[e]	—	—	—	—	—	—
	352	245	81	114	0	18	99	186	89	19	29	0	108
RhNaY	328	35	55	61	0	4	59	32	44	6	—	0	50
Rh/Al_2O_3	328	500	170	181	24	25	219	384	196	26	76	0	222

[a] CO (48 ± 2 Torr), H_2 (51 ± 5 Torr), and H_2O (18 ± 2 Torr) were separately reacted.
[b] Measured from CO_2 formed by the disproportionation reaction.
[c] Total amount of CO_2 and CH_4 obtained by the recirculation of H_2 and H_2O.
[d] Evacuated for 1 h after the disproportionation reaction; the normal time was 5 min.
[e] Temperature increase to 400°C in a hydrogen atmosphere resulted in the appearance of CH_4 (40 μmol/g).

extrapolation to zero time the initial activity was evaluated. The TOF for the WGS reaction as of function of the initial carbon coverage over this series of catalyst is plotted in Fig. 8. Here it is evident that a reasonable correlation exists between the initial surface coverage of carbon and the activity for the WGS reaction.

These results, together with the order of the reaction with respect to CO, suggest that surface carbon plays an important role in WGS reaction over supported rhodium via a mechanism of the type:

$$CO + 2s \rightleftarrows C_a + O_a, \quad (5)$$

$$H_2O + 2s \rightleftarrows OH_a + H_a, \quad (6)$$

$$C_a + OH_a \rightleftarrows CO_a + H_a, \quad (7)$$

$$CO_a + O_a \rightleftarrows CO_2 + 2s, \quad (8)$$

$$2H_a \rightarrow H_2 + 2s, \quad (9)$$

where s denotes a surface site. If reaction (7) is rate limiting, the predicted reaction orders would be −0.5 and 0.5 for CO and H_2O, respectively, for the case where CO is strongly adsorbed. By contrast, for the WGS reaction over supported Ru catalysts

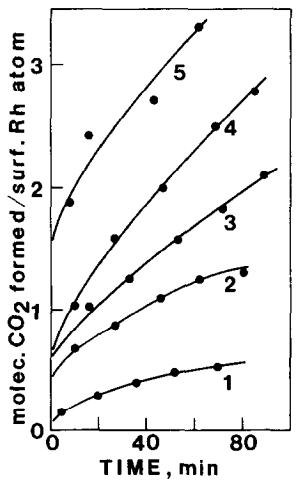

FIG. 7. Molecules of CO_2 per surface Rh atom during disproportionation of CO at 328°C: (1) RhNaY, (2) 4 wt% Rh/Y, (3) Rh/SiO_2, (4) 2 wt% Rh/Y, (5) Rh/Al_2O_3.

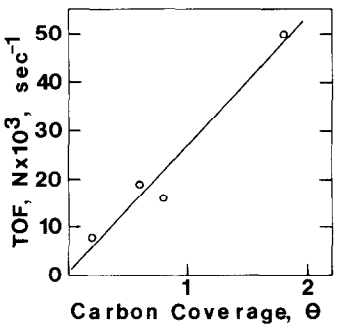

FIG. 8. Turnover frequency for WGS reaction as a function of initial carbon coverage.

the evidence favored a reaction between molecular CO_a and OH_a rather than reaction (7).

The TOF for the WGS over RuY, extrapolated to the conditions listed in Table 3, was 0.36, which is more than an order of magnitude greater than the values obtained for the RhY catalysts. This relative activity is in contrast with the conclusions of Joy *et al.* (*35*), who found that rhodium was more active than ruthenium on an automotive-type support with a gas mixture typical of those found in an automotive exhaust.

With both RhY and supported Ru catalysts the WGS reaction is sufficiently rapid so that the steady-state concentration of surface carbon is small. Methane is the exclusive hydrocarbon product since FT reactions to form higher hydrocarbons require bimolecular reactions involving carbon intermediates (*36*). The selective formation of methane during the hydrogenation of CO_2 over supported rhodium has likewise been attributed to the limited amount of carbon on the surface (*29*). Rhodium on alumina behaves differently because of its superior ability to dissociate CO, and consequently ethane is also a product. Apparently ethane was removed in the recirculating reactor (Fig. 5) by a hydrogenolysis reaction.

CONCLUSIONS

(1) Over supported rhodium CH_4 formation from CO and H_2O occurs via the water gas shift reaction followed by the hydrogenation of surface carbon. There is no evidence to support the direct reaction of H_2O with CO or surface carbon to form CH_4.

(2) The rate of the water gas shift reaction is proportional to the ability of supported rhodium to form surface carbon, which varies with the type of support. The dissociation of CO may, in turn, be related to the concentration of surface defects on the metal crystallite. By contrast, over supported ruthenium the reaction involves only molecular CO, thus the dissociation reaction is not important, and the effect of the support is less a factor.

(3) As a practical matter extensive conversion of CO and H_2O to CH_4 and CO_2 can be achieved over supported rhodium catalysts by operating at sufficiently high temperatures and W/F values. Rhodium on the external surface of a Y-type zeolite was the most effective catalyst among those studied.

ACKNOWLEDGMENT

The authors wish to acknowledge the support of this work by the Division of Basic Energy Sciences, Department of Energy, and Center for Energy and Mineral Resources, Texas A&M University.

REFERENCES

1. Kölbel, H., and Bhattocharyga, K. K., *Leibigs Ann. Chem.* **618,** 67 (1958).
2. Smith, A. K., Theolier, A., Basset, J. M., Ugo, R., Commereuc, D., and Chauvin, Y., *J. Amer. Chem. Soc.* **100,** 2590 (1978).
3. Brenner, A., and Hucul, D. A., *J. Amer. Chem. Soc.* **102,** 2484 (1980).
4. Gustafson, B. L., and Lunsford, J. H., *J. Catal.* **74,** 393 (1982).
5. Udrea, I., Moroianu, M., Udrea, M., and Nicolescu, I. V., "Heterogeneous Catalysis Proceedings 4th Int. Symp., Varna, 1979.
6. Vannice, M. A., *Catal. Rev. Sci. Eng.* **14,** 153 (1976).
7. Niwa, M., Iizuka, T., and Lunsford, J. H., *J. Chem. Soc. Chem. Commun.*, 684 (1979).
8. Castner, D. G., Dubois, L. H., Sexton, B. A., and Somorjai, G. A., *Surf. Sci.* **103,** L134 (1981).
9. Dalla Betta, R. A., *J. Catal.* **34,** 57 (1974).
10. Scofield, J. H., *J. Electron. Spectrosc.* **8,** 129 (1979).
11. Iizuka, T., and Lunsford, J. H., *J. Mol. Catal.* **8,** 391 (1980).
12. Okamoto, Y., Ishida, N., Imanaka, T., and Teranishi, S., *J. Catal.* **58,** 82 (1979).
13. Yao, H. C., Japar, S., and Shelef, M., *J. Catal.* **50,** 407 (1977).
14. Wagstaff, N., and Prins, R., *J. Catal.* **59,** 434 (1979).
15. Bergeret, G., Gallezot, P., and Imelik, B., *J. Phys. Chem.* **85,** 411 (1981).
16. Contour, J. P., Mouvier, G., Hoogewys, M., and Leclere, C., *J. Catal.* **48,** 217 (1977).
17. Primet, M., Vedrine, J. C., and Naccache, C., *J. Mol. Catal.* **4,** 411 (1978).
18. Yang, A. C., and Garland, C. W., *J. Phys. Chem.* **61,** 1505 (1956).
19. Yao, H. C., and Rothschild, W. G., *J. Chem. Phys.* **68,** 4774 (1978).

20. Yates, D. J. C., Murrell, L. L., and Prestridge, E. B., *J. Catal.* **57,** 41 (1979).
21. Primet, M., *J. Chem. Soc. Faraday Trans. 1* **74,** 2570 (1978).
22. Smith, A. K., Hughes, F., Theolier, A., Basset, J. M., Ugo, R., Zanderighi, G. M., Bilhou, J. L., Bilhou-Bougnool, V., and Graydon, W. F., *Inorg. Chem.* **18,** 3104 (1979).
23. Gelin, P., BenTaarit, Y., and Naccache, C., *J. Catal.* **59,** 357 (1979).
24. Gallezot, P., *Catal. Rev. Sci. Eng.* **20,** 121 (1979).
25. Verdonck, J. J., Schoonheydt, R. A., and Jacobs, P. A., "Preprints, Seventh Int. Congr. Catal., Tokyo, 1980;" Verdonck, J. J., Jacobs, P. A., and Uytterhoeven, J. B., *J. Chem. Soc. Chem. Commun.*, 181 (1979).
26. Vannice, A., *J. Catal.* **37,** 449 (1975).
27. Dalla Betta, R. A., Piken, A. G., and Shelef, M., *J. Catal.* **35,** 54 (1974).
28. Elliott, D. J., and Lunsford, J. H., *J. Catal.* **57,** 11 (1979).
29. Solymosi, F., Erdöhelyi, A., and Bansagi, T., *J. Catal.* **68,** 371 (1981).
30. Rabo, J. A., Risch, A. P., and Poutsma, M. L., *J. Catal.* **53,** 295 (1978).
31. Yates, J. T., Williams, E. D., and Weinberg, W. H., *Surf. Sci.* **91,** 562 (1981).
32. Sexton, B. A., and Somorjai, G. A., *J. Catal.* **46,** 167 (1977).
33. Gustafson, B. L., and Lunsford, J. H., *J. Catal.* **74,** 405 (1982).
34. Gupta, N. M., Kamble, V. S., Annaji Rao, K., and Iyer, R. M., *J. Catal.* **60,** 57 (1979).
35. Joy, G. S., Molinavo, F. S., Lester, G. R., Paper presented at 6th North American Catalysis Society Meeting, March, 1979.
36. Ponec, V., *Catal. Rev.-Sci. Eng.* **18,** 151 (1978).